Four-terminal perovskite/c-Si tandem PV technology

Dong Zhang[1], Stefan Luxembourg[2], Gianluca Coletti[2], Sjoerd Veenstra[1] & Bart Geerligs[2]
[1]ECN part of TNO – Solliance, Eindhoven; [2]ECN part of TNO, Petten, The Netherlands

Abstract

Two factors have coincided to stimulate the recent spur in interest for hybrid tandem PV technology based on crystalline silicon – the fact that balance-of-system (BOS) costs are increasingly dominating turnkey system costs, which strengthens the effect of high efficiency in reducing Wp costs, and the discovery of perovskite solar cells as a promising low-cost wide-band-gap partner for crystalline silicon (c-Si). This paper presents the progress and analysis of four-terminal (4T) perovskite/c-Si tandem technology at ECN part of TNO, with perovskite technology development carried out within the Solliance research organization. Tandem cell optimization and optical loss analysis are presented, with the combination of high efficiency and high near-infrared (NIR) transmittance of the perovskite cell resulting in an experimental tandem efficiency of 26.3%. An outlook is offered for loss reduction and efficiency increase. Upscaling and interconnection of the perovskite cell are crucial aspects for industrialization, and the status at Solliance is briefly described. High-end c-Si bottom cells are then compared with mainstream industrial cells; how industrial PERC and nPERT cells can be optimized for tandem application is described, as well as even making them suitable for two-terminal tandem application, through the application of polysilicon (polySi) passivated contacts. Finally, this paper looks at the cost of tandem versus single-junction (SJ) c-Si systems, and shows that the recent literature on perovskite module manufacturing cost is consistent with a potential cost advantage of tandem devices.

Introduction

As the balance-of-system (BOS) costs begin overtaking the solar module cost in the turnkey PV system cost [1], the role of the efficiency of the PV module becomes increasingly important in reducing the levelized cost of electricity (LCOE) from PV. Additionally, the ambition for strong further growth in PV generation capacity, and the controversy this already causes in more densely populated regions (e.g. large parts of Europe) with regard to making land area available for PV system deployment, favour the development of higher-efficiency PV modules. *Tandem PV technology* which combines bottom crystalline silicon (c-Si) cells with low-cost wide-band-gap thin-film top cells is expected to enable major increases in efficiency to be made and could therefore contribute significantly in these respects.

Of the thin-film PV technologies, the perovskite solar cell is considered a promising candidate for the top cell. Modelling has shown that an optimized perovskite/c-Si tandem configuration can result in a large efficiency increase over single-junction (SJ) c-Si cells [2]. In fact, several researchers have calculated that it should be possible for the efficiency of perovskite/c-Si tandem cells to exceed 30%, which is definitely out of reach for SJ c-Si cells [3,4]. Over the last three years, much progress has been made in the field of perovskite/c-Si tandem cells (Fig. 1) [5]. A cell efficiency as high as 26.9% has been demonstrated for a four-terminal (4T) tandem cell [6], and 25.0% has been announced for a monolithic two-terminal (2T) perovskite/c-Si tandem cell [7].

Compared with the 2T configuration, the use of a 4T tandem cell configuration (Fig. 1) has certain advantages: for example, the absence of a current matching constraint, and the possibility for module construction from separately manufactured and tested submodules or submodule strings. On

Figure 1. (a) Evolution of perovskite/c-Si tandem record efficiencies. (b) Schematic layout of 2T and 4T tandem cell configurations.
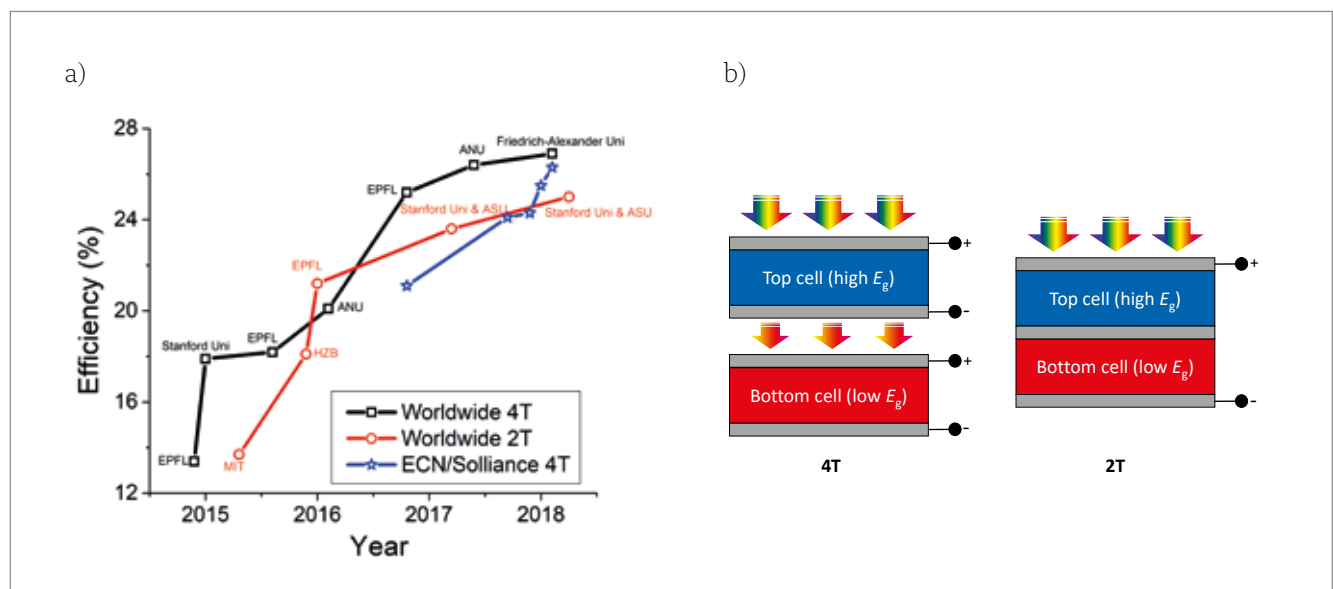
"Tandem PV technology is expected to enable major increases in efficiency to be made."

the other hand, the electrical wiring and system integration of the 4T module will be more complex, and the required transparent conductive layer with low sheet resistance on the rear side of the perovskite top cell (PTC) may result in significantly increased near-infrared (NIR) absorption loss. It seems that the R&D community and industry have not yet reached a consensus on a preference for 2T or 4T configurations, with both being actively investigated. This paper presents the progress made by Solliance and by ECN part of TNO on the development of 4T perovskite/c-Si tandems. In the research organization Solliance, of which ECN part of TNO is one of the partners, the semi-transparent perovskite device is under development, while ECN part of TNO is focusing on the c-Si cell aspects
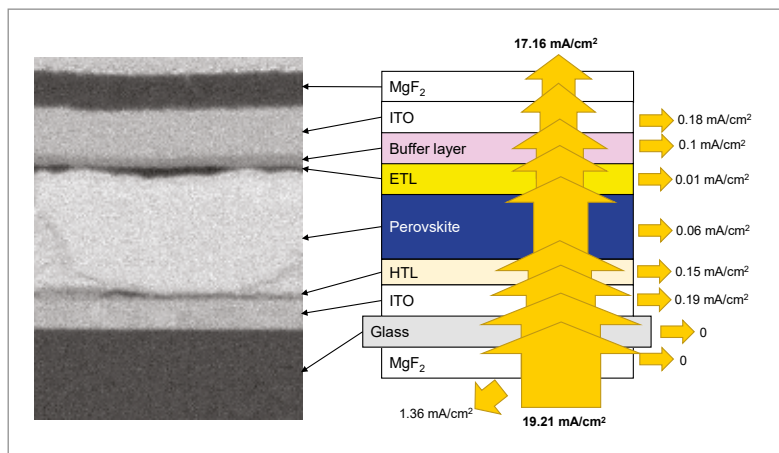
and the integration of both components in hybrid tandem modules.

Perovskite/c-Si tandem cell results

One of the biggest challenges in achieving high tandem cell efficiency is the NIR transmission of the PTC. Considering the state-of-the-art c-Si cells with an external quantum efficiency (EQE) that can approach 100% [8], a limited NIR transmittance of the PTC inevitably induces large optical losses in the c-Si bottom cell. This limitation is especially relevant for 4T tandems, in which the PTC has to utilize two semi-transparent electrode layers, as these are the main causes of NIR parasitic absorption losses.

A transparent perovskite cell with a very high average NIR transmittance of 93%, developed with laboratory processes at Solliance, is shown in Fig. 2; the development of this cell has been described in detail in several publications [9–11]. The perovskite absorber layer, the organic selective contact layers, and the metal oxide charge transport layers are deposited by spin coating. The ZnO buffer layer to protect the perovskite from sputter damage is deposited by spatial atomic layer deposition (ALD), and the tin-doped indium oxide (ITO) layers are deposited by sputter coating. Thermally evaporated MgF_2 layers are added to reduce the front reflection, and also the internal reflection at the back side of the cell (in mass production, the front of the cell would have a regular anti-reflection (AR) coating, and the internal reflection at the rear would be reduced by the presence of an encapsulant).

The optical loss analysis for the 800–1,200nm NIR wavelength range is shown on the right in Fig. 2; this analysis uses the optical constants of the individual layers as determined by reflection/transmission measurements and spectroscopic ellipsometry. A key aspect of the development of this highly NIR-transparent PTC was the precise tuning of the oxygen partial pressure during the deposition of the

Figure 2. Cross-sectional scanning electron microscope (SEM) image of perovskite solar cell (left) developed at Solliance for use in 4T tandem cells, and its optical loss analysis (right) for the NIR region (800–1,200nm) of the AM1.5 spectrum (ETL = electron transport layer, HTL = hole transport layer) [9–11].
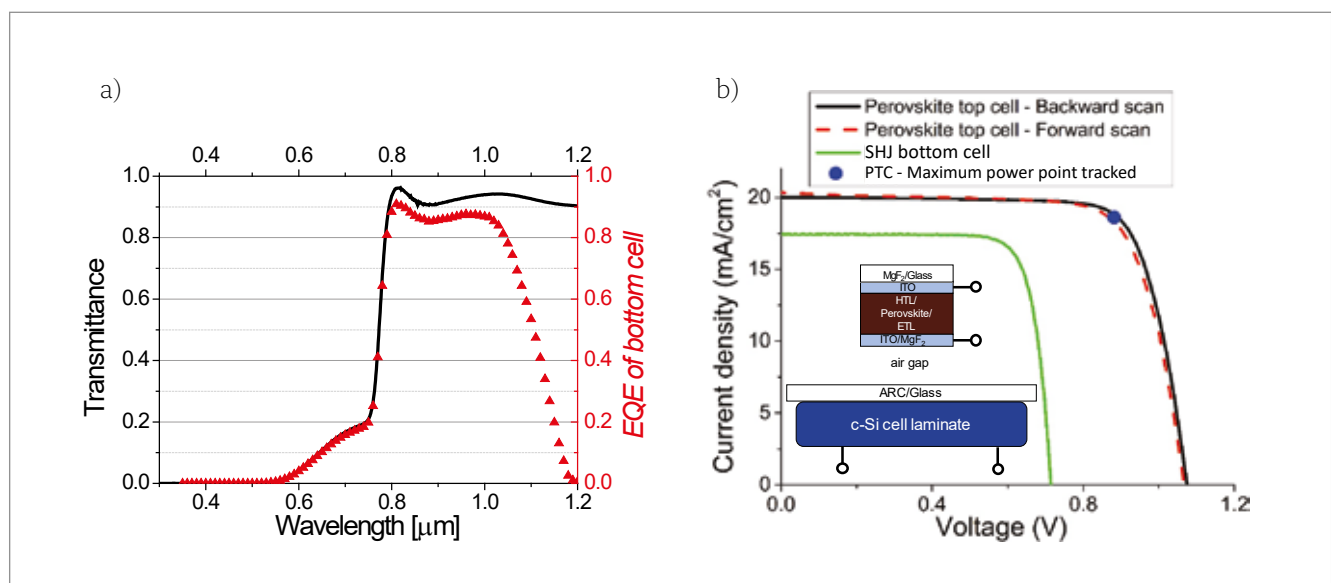

Figure 3. Best 4T tandem result obtained at ECN/Solliance: (a) transmittance of the PTC (black), and the filtered EQE of the c-Si SHJ cell (red) [12]; (b) I–V characteristics of the top and bottom cells (the inset shows schematically the configuration of this 4T tandem device).

Cell type		V_{oc} [V]	J_{sc} [mA/cm^2]	FF	η [%]
Perovskite top cell (Fig. 2)	Backward scan	1.075	20.0	0.772	16.6
	Forward scan	1.067	20.3	0.746	16.2
	MPPT 5 min.				16.4
C-Si silicon heterojunction (SHJ) cell [12]	Single-junction	0.731	39.8	0.781	22.7
	Bottom cell	0.714	17.3	0.796	9.9
Tandem cell					26.3

Table 1. Efficiency measurement of the 4T perovskite/c-Si tandem cell in Fig. 3 (MPPT = maximum-power-point tracked). (In-house measurements, taken according to the procedure outlined in Werner et al. [13].)

ITO layers, in order to control the concentration and type of defects. This allowed a high value for the product of mobility and carrier density, at relatively low carrier density, resulting in the very high NIR transmittance (Fig. 3).

The PTC described above was combined with a laminated high-efficiency silicon heterojunction (SHJ) cell [12]. Because of the difference in size of the PTC (3×3mm^2 aperture area) and the c-Si cell (243cm^2), the 4T tandem efficiency was determined on the basis of the filtered EQE measurement of the c-Si cell, as described by Werner et al. [13]. The results are shown in Fig. 3 and Table 1.

The optical analysis shows that the major remaining optical losses in this tandem stack consist of:
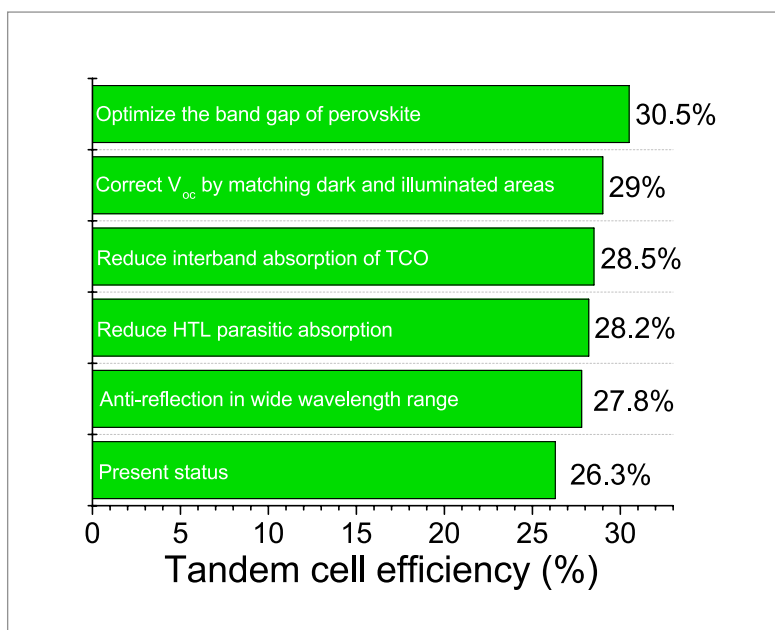· Reflection: ~3.7mA/cm^2
· Absorption in the HTL and ETL of the perovskite cell stack: ~0.9mA/cm^2
· UV (inter-band) absorption in the front ITO: ~0.8mA/cm^2
· Free-carrier absorption (FCA) in the ITO: ~0.4mA/cm^2

There is a lot of room for improvement in the 4T tandem cell efficiency by further development and optimization. Fig. 4 shows how a significant increase in efficiency is possible through various enhancements, such as reductions in reflection and parasitic absorption losses, and tuning of the perovskite band gap. It is expected to be possible to achieve in practice a tandem cell efficiency of over 30% with the same c-Si cell as in Table 1.

Scalability of the perovskite process technology, and device stability
The prospect of perovskite/c-Si tandem solar cells enabling mainstream PV technology (c-Si) to enter a new efficiency regime is appealing, given the efficiency results and the outlook described above. To turn this prospect into reality, high efficiency in itself is not sufficient; it is equally important for tandem devices to be as stable as c-Si modules. In addition, industrial processes need to be in place for producing efficient and stable hybrid tandem devices on a large scale and at a low cost, leading to a competitive levelized cost of electricity (LCOE).

It is important to note the typical difference in cell dimensions between the perovskite top cell and the c-Si bottom cell in the current laboratory 4T tandem cells, a factor already touched upon in the previous

Figure 4. Outlook for improvements in the optical properties of the PTC, and thus in the perovskite/c-Si tandem cell efficiency, and for a further efficiency increase by optimizing the perovskite band gap. The V_{oc} improvement by matching dark and illuminated areas refers to avoiding the V_{oc} loss that is observed in the PTC due to the measurement aperture being smaller than the cell area. The cell V_{oc} was demonstrated to be higher at the module level [9–11].

section. The cell area of highly efficient perovskite top cells is often between 0.1 and 1cm^2, whereas the cell area of industrial c-Si cells is typically (6")^2, which is two to three orders of magnitude larger. Importantly, when the cell dimensions increase, the generated photocurrent increases, leading to ohmic losses in the semi-transparent electrodes. This issue can be mitigated by introducing a current-collecting metal grid, or by dividing the cell area into a number of smaller sub-cells and electrically interconnecting these sub-cells in series. In the latter case, the current flowing through the PV device is reduced and the voltage concurrently increased. Almost all commercial thin-film PV modules are based on this concept of monolithically serially interconnected cells. The optimized width of a unit cell in a serially interconnected perovskite module for a 4T tandem configuration is between 3 and 5mm, depending on the applied semi-transparent electrodes, the photocurrent density and the required area for serial interconnection [14,15]. The area taken up by the serial interconnection, while not contributing to power generation in the perovskite module, can be as transparent as the other areas of the PTC stack, and

"High efficiency in itself is not sufficient; it is equally important for tandem devices to be as stable as c-Si modules."

can therefore contribute to power generation in the bottom c-Si module.

Consequently, by using small perovskite cells in R&D, the cell width of an optimized sub-cell in a monolithically interconnected module can be represented, without the need for already introducing an interconnection scheme in the device. As a next step, efficient 'area-matched' 4T tandem devices have now recently also been reported; these are based on stacking a perovskite module on a small c-Si cell, with a device area exceeding 1cm² [16].

In order to prepare semi-transparent perovskite modules matching the size of commercially relevant 6" c-Si cells or even standard ~1.6m² c-Si modules, scalable industrial deposition methods – such as slot die coating, spray deposition, inkjet printing or physical vapour phase deposition – should be employed. An initial challenge is to reproduce with the scalable deposition method the efficiency of the non-scalable deposition method on small-size cells. Fig. 5 proves the feasibility of replacing spin coating by slot die coating to deposit the perovskite layer or selective charge transport layer, without significant loss in performance [17].

Another aspect of identifying suitable scalable processes for large-area deposition of perovskite layers is the use of solvents which can be employed in an industrial setting [18]. Although several laboratory-scale deposition processes have been developed for perovskite solar cells, the most frequently used wet-chemical method involves the deposition of the perovskite precursors by spin coating in a single step, followed by the application of a second solvent [19]. The second solvent (also called *anti-solvent*) causes rapid supersaturation in the drying, but still wet, film, resulting in a uniform, smooth, high-quality perovskite layer. The accurate timing of the application of the second solvent (after

the deposition of the perovskite precursor solution) is crucial. This procedure, however, is not by any means easily transferable to an industrial setting.

Several research groups have developed more industrially relevant processes by engineering the solvent system [20], or by using a strong air flow to quench the crystallization process [21]. At Solliance, the development of these processes has recently led to the realization of 6" SJ perovskite modules prepared with scalable deposition methods, with efficiencies of 13.8% on the aperture area and 14.5% on the active area (Fig. 6) [22].

The typical absorber materials used in perovskite solar cells are not as resistant to external stress factors as silicon. Nevertheless, by the application of stable layers contacting the perovskite layer, and by preventing ingress and even egress of chemical components by the application of gas barrier layers, several groups have now reported stable device performance under prolonged illumination (1,000h, 1 sun equivalent) or with exposure to elevated temperatures (1,000h, 85°C), without suffering more than a 10% drop in performance. These results show that if the perovskite solar cell is well packaged, it can be stable when exposed to light and elevated temperatures and can pass the IEC damp-heat test [23].

Choosing and optimizing c-Si bottom cells for tandem application

The c-Si bottom cells most often used in studies of perovskite/c-Si tandem cells are high-performance cells, in particular interdigitated back contact (IBC) and amorphous-silicon/c-Si heterojunction (SHJ) cells. For the large-scale production of perovskite/c-Si tandem PV, it could make more economic sense to use lower-cost bottom cells; the reason for this is that increasing the efficiency of the bottom cell will not translate directly to the same efficiency gain in the full tandem stack. As a result, the process
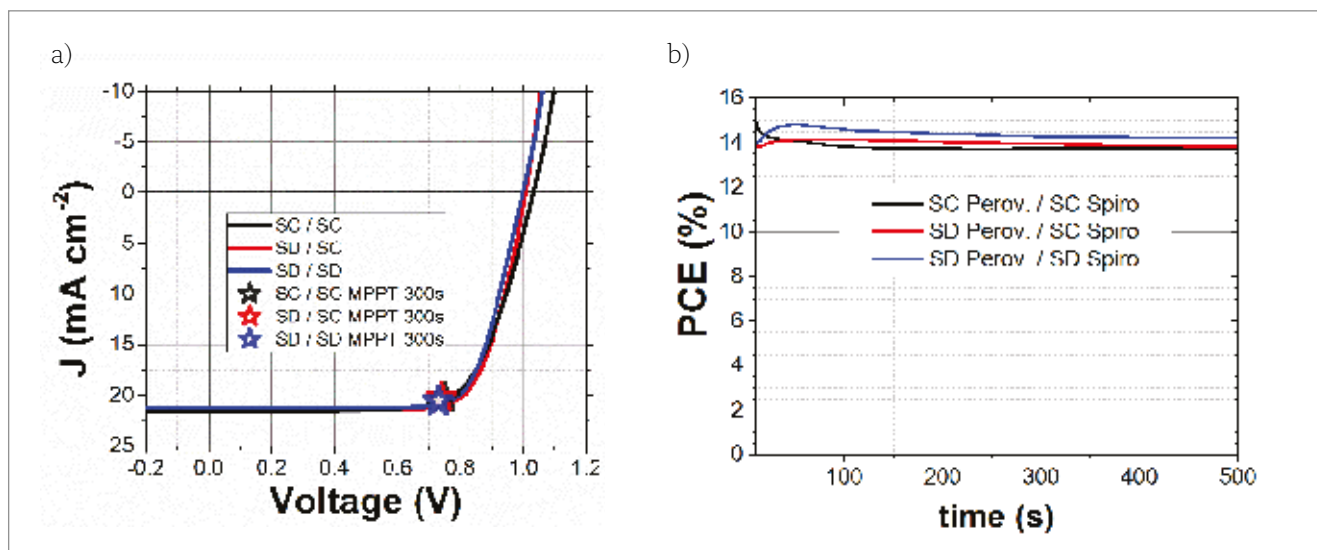

Figure 5. Illustration of the feasibility of replacing spin coating (SC) by scalable slot die (SD) coating technology in perovskite cell processing: (a) typical J–V curve of the perovskite cells; (b) typical maximum-power-point tracking (MPPT) curves for the devices, measured under maximum-power-point voltage bias, from Di Giacomo et al. [17]. (Perov. = perovskite absorber layer; Spiro = spiro-OMeTAD charge contact layer.) Reprinted with permission from Di Giacomo et al. [17].

costs for a higher-efficiency c-Si bottom cell will be greater in terms of added $/W for the tandem stack than those for the c-Si cell alone.

The filtered performance of c-Si cells (i.e. the performance in a tandem stack) depends on the transmittance of the perovskite stack, as well as on the c-Si cell properties, such as EQE, V_{oc} loss under reduced irradiation, and shunt and series resistances. Fig. 7 and Table 2 show a comparison of the performance of several c-Si cells, relevant to industrial mass production, for tandem application.

Fig. 7 shows the spectral efficiency [4] of various industrial and industrially relevant c-Si cells. The spectral efficiency incorporates the V_{oc} and fill factor (*FF*) determined under reduced irradiation to correspond to the filtered J_{sc}. Typically, it is found that V_{oc} scales with irradiation according to the diode equation with an ideality factor close to unity (i.e. about 22mV loss under the ~1.6eV perovskite stack), and that *FF* increases because of the reduction in series resistance loss. The contribution to tandem cell efficiency can be estimated from the product of the spectral efficiency, the transmittance of the perovskite stack, and the photon power density in the AM1.5 spectrum, integrated over the photon wavelength. The resulting *I–V* parameters of the filtered c-Si cells are given in Table 2.

Table 2 shows that the efficiency benefit under AM1.5 of the SHJ over the nPERT cell is halved in tandem application. The Al-BSF cell has significantly worse spectral efficiency for NIR wavelengths, and therefore shows a comparatively large reduction in efficiency in filtered operation (e.g. filtered efficiency 1.0% lower than a PERC cell, compared with 1.6% lower efficiency under AM1.5). In addition to the more established industrial cells, Fig. 7 shows the results for an nPERT cell employing polysilicon (polySi) passivated contacts on the front and rear sides, instead of a diffused emitter and back-surface field (BSF); this use of polySi passivated contacts is discussed in detail in the next section. In the context of selecting the bottom cells, it should be noted that in a 4T tandem cell design, the J_{sc}s of the top and bottom cells do not need to be matched as in the case of the 2T design; as a result, a 4T design based on bifacial c-Si cells will enable bifacial modules with the associated energy yield benefit.
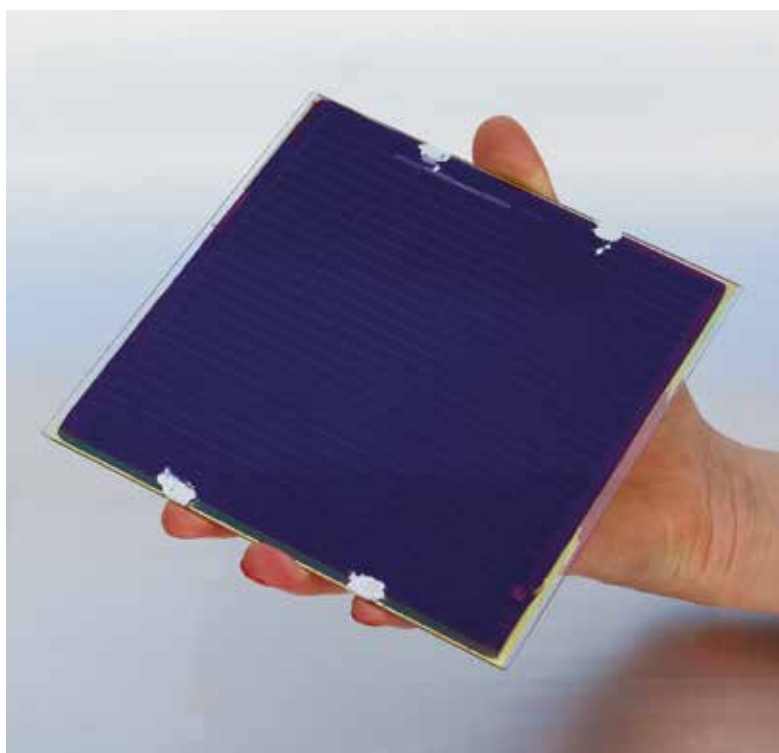
Figure 6. A 6" × 6" perovskite module processed by slot die coating, laser interconnection and encapsulation with a barrier film [17].
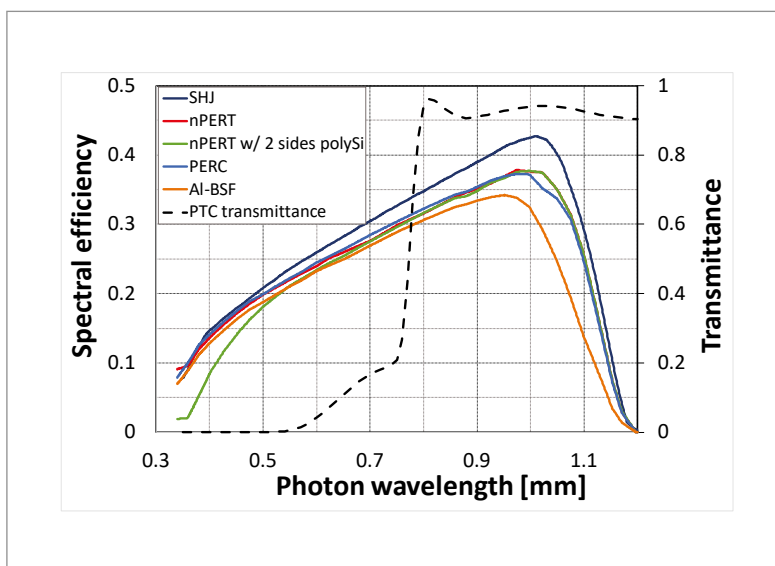
Figure 7. Spectral efficiencies of several types of industrial or industrially processed c-Si cells (solid lines). The transmittance of the perovskite cell stack described in the perovskite/c-Si tandem cell results section is indicated by the dashed line.

Cell type	AM1.5				Filtered				
	V_{oc} [V]	J_{sc} [mA/cm²]	*FF*	η [%]	V_{oc} [V]	J_{sc} [mA/cm²]	*FF*	η [%]	J_{sc} ratio
SHJ	0.731	39.8	0.781	22.7	0.714	17.3	0.796	9.9	0.436
nPERT	0.664	39.4	0.793	20.7	0.642	16.8	0.813	8.8	0.426
PERC	0.670	39.6	0.807	21.4	0.647	16.7	0.813	8.8	0.422
nPERT with polySi both sides	0.685	38.2	0.765	20.0	0.656	17.0	0.785*	8.8	0.445
Al-BSF	0.640	38.2	0.810	19.8	0.615	15.6	0.812	7.8	0.407

*estimated

Table 2. Single-junction efficiency and contribution to tandem cell efficiency for different types of c-Si cell. The SHJ cell is laminated with AR-coated glass; the other cells are unlaminated.

"The implementation of a polySi contact can be achieved with only a minor addition to the regular process flow."

PolySi passivated contacts on the bottom cell

In SJ c-Si solar cells, much attention has recently been directed at the implementation of extremely carrier-selective contacts, which, because of their low contact recombination, enhance the voltage and efficiency of the solar cell. In particular, a stack of thin oxide and a doped polySi layer is considered a practical and useful carrier-selective contact, which has enabled the realization of a cell efficiency higher than 25% [24,25]. Recombination current pre-factors (J_o) of less than 1fA/cm^2 have been achieved for n-type polySi; moreover, even fire-through metal paste contacts, while not fully passivated, can result in relatively low recombination current pre-factors of well below 500fA/cm^2 for the metallized area.

When aimed at SJ c-Si cell use, polySi is applied onto the back of the solar cell, since the significant number of carriers which are generated in a front-side polySi layer by short wavelength photons are generally not collected in the wafer, but instead lost to recombination. NIR wavelengths are, however, mainly transmitted through a front polySi layer to the c-Si wafer. A front polySi contact therefore shows less parasitic absorption when applied onto a c-Si bottom cell in tandem application, while it enhances cell performance through its low recombination. This phenomenon is illustrated in Table 2 by a comparison of the regular nPERT and the nPERT with a polySi contact layer on both sides; the two devices have similar J_{sc}s, but the V_{oc} is significantly boosted in the case of the nPERT with polySi passivated contacts.

A particular benefit of a polySi front contact is that it is expected to be suitable for 2T tandems, since the polySi passivating layer is conductive, in contrast to traditional passivating layers which are dielectric. In this respect, c-Si cells with a polySi front contact are an attractive alternative to SHJ cells, enabling high-temperature processed mainstream industrial cells to be adapted for use in 2T tandems.

Apart from nPERT cells with front and rear polySi contacts [26], the development of PERC cells with a front polySi contact (poly PERC, Fig. 8, [27]) has also begun. In both cases, the implementation of a polySi contact can be achieved with only a minor addition to the regular process flow (primarily the deposition of the oxide/polySi stack), and therefore with minor, if any, additional cost to the c-Si cell process.

Two types of parasitic absorption are of importance for bottom cells using a front polySi contact layer: 1) parasitic band-to-band absorption of the short wavelengths transmitted through the top cell; and 2) parasitic FCA of the long wavelengths. The parasitic band-to-band absorption is determined by the thickness of the polySi, the band gap of the perovskite, and the transmission shoulder at the absorption edge due to the finite thickness of the perovskite. The FCA is determined by the doping level and optical properties (effective path length) of the bottom cell. Qualitatively, the effect of the band-to-band absorption is clearly observable in the EQE and spectral efficiency (see, for example, Fig. 7). A ray-tracing model analysis was used to quantify the losses, on the basis of the optical properties of the perovskite stack described in the perovskite/c-Si tandem cell results section, with a shift of the refractive index and extinction coefficient curves of the perovskite layer over 0.15 and 0.35eV to model the wider band gap perovskites. The results are shown in Fig. 9.

The band-to-band absorption loss shown in Fig. 9 will decrease if the transmission shoulder of the perovskite is reduced (for example, if a thicker perovskite layer is used). In addition, for a 2T tandem cell application, the polySi layer thickness can be reduced, since the polySi does not need to provide lateral current transport.

The FCA loss depends on the doping level, which, for a certain required sheet resistance, depends on the mobility in the polySi. In practice, the mobility in n-type polySi is around half to one-third that in equally doped crystalline silicon, depending on the
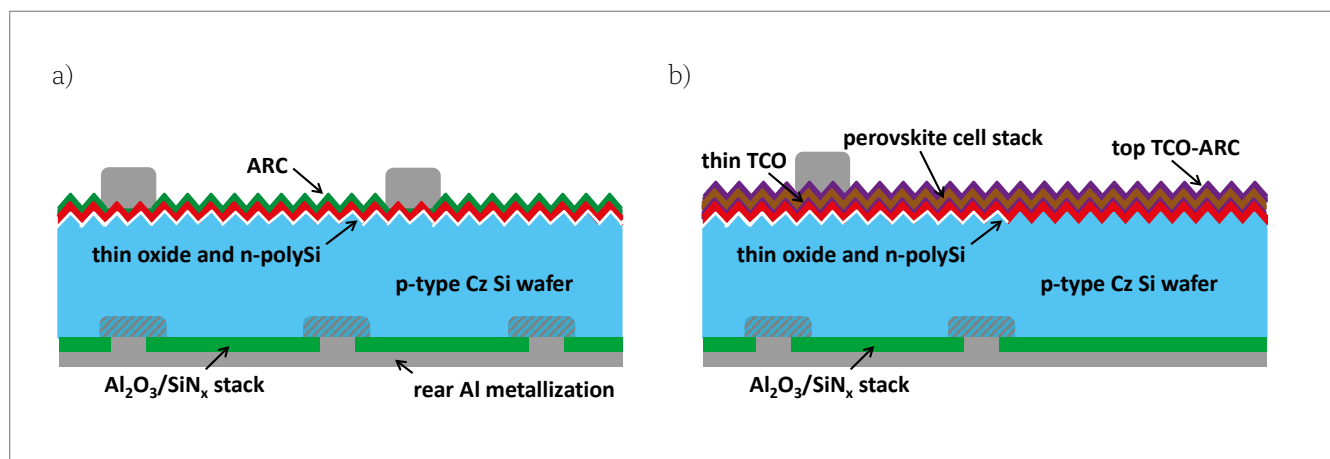

Figure 8. Schematic of the application of a polySi passivated contact in a bottom cell for a tandem stack in: (a) a PERC cell for 4T tandem application; (b) a possible 2T tandem layout based on the same cell concept.

exact process conditions [28]. Compared with a poly PERC cell, for an nPERT cell additional FCA is caused by the presence of a p-type polySi layer. While this seems to favour a PERC cell design (unless bifacial operation is required), the experimental results in Table 2 do not bear out the significantly large differences in the modelled FCA between PERC and nPERT. Further experimental and model analysis may be required in order to clarify this.
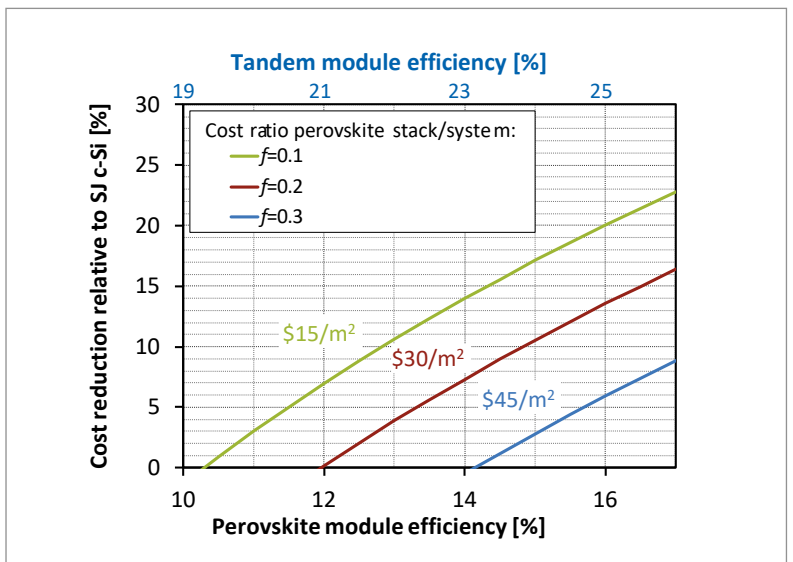
Cost

One of the principal arguments for tandem PV is the increase in efficiency, which will reduce the contribution of area-related module and system costs to the cost per Wp and the cost per kWh (LCOE). By virtue of this effect, tandem PV can potentially become more cost-effective than SJ PV, despite the additional cell process costs.

If the reference SJ (c-Si) turnkey system cost is $1/Wp, a one percentage point efficiency gain for a tandem module over the c-Si bottom submodule will have a value of roughly $10/m^2, when neglecting the increase in Wp-related BOS costs. If the best laboratory results for the efficiency gain of around 4–5% (see the perovskite/c-Si tandem cell results section) of tandem cells over mainstream industrial cells can be maintained at the module level, this would then represent a value of about $40–50/m^2. This estimate for cost-effectiveness, and the cost reduction that can be achieved at the system level, are illustrated in a more generalized way in Fig. 10. Details of the model, sensitivities, etc. are given in Geerligs [29]; the work reported in this reference also considers the relation between system cost comparison and LCOE comparison, noting the possible changes in thermal effects (operating temperature, temperature coefficient), and in degradation (a relative efficiency degradation of 1%/year would increase the LCOE by more than 10%, the same order of magnitude as the potential system cost advantage in Fig. 10).

Several studies on the anticipated cost of perovskite module production have recently been published. The cost estimates in these studies vary widely: for example, the estimates of the manufacturing cost of the transparent conducting oxide (TCO) layers vary between $3/m^2 [30] and more than $9/m^2 [31]. Some published manufacturing cost estimates are listed in Table 3, in which the cost of a metal electrode, if assumed to be in the stack, has been replaced by the cost of a second TCO electrode.
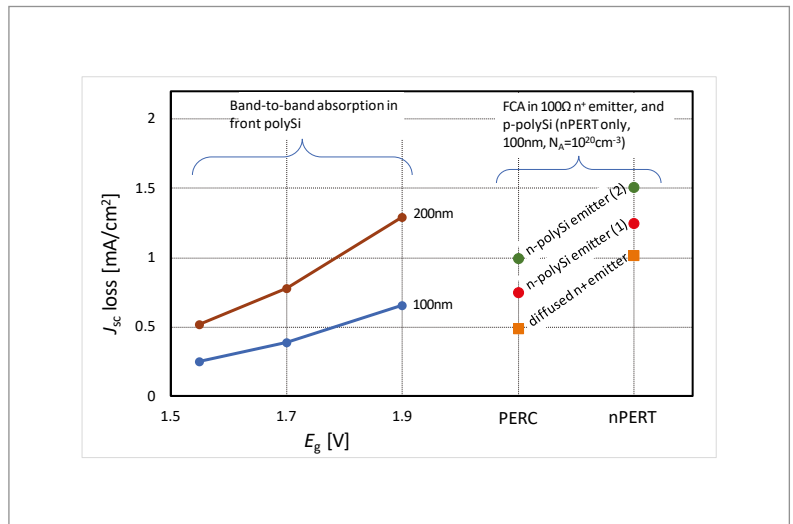
Figure 9. Ray-tracing model results of the parasitic absorption in c-Si bottom cells. Left graph: band-to-band absorption in a polySi passivating contact on the front of a c-Si bottom cell, as a function of the perovskite band gap. Right graph: FCA in PERC and nPERT cells with a 100Ω/sq. front emitter – a diffused emitter, a polySi emitter with half the mobility of crystalline silicon (1) or a polySi emitter with one-third the mobility (2). For example, the polySi emitter (1) has an n-type doping concentration of 1.6×10^{20}cm^{-3} over a thickness of 100nm.

Figure 10. Illustration of the system cost reduction for a perovskite/c-Si tandem PV system, relative to a c-Si SJ PV system with 18% module efficiency, as a function of the cost for adding the perovskite stack (including, if relevant, changes in module materials, system cabling, power electronics, etc.). The parameter f is the ratio of this perovskite stack cost to the total SJ system cost, and the coloured labels show the approximate translation to a stack cost in $/m^2 in the case of a SJ system cost of $1/Wp. A filtered c-Si module efficiency of 9% in a tandem configuration is assumed in this calculation, roughly appropriate for a perovskite band gap of 1.7eV. Model details are given in Geerligs [29].

Reference/year	Perovskite stack [$/m^2] [a]	Complete module [$/m^2]	Stack structure
[32]/2015	25.5	55	ITO/TiO$_2$ scaffold/perovskite/Spiro/ITO
[31]/2017	Not specified separately	≥50 [b]	ITO/PEDOT:PSS/perovskite/PCBM/Ca/Al
[30]/2017	9±1 [b]	34±5 [b]	ITO/NiO/perovskite/ZnO/Al

[a]Including monolithic interconnection and busbar contacts.
[b]The cell stack includes a rear metal electrode; the cost of this metal electrode was therefore replaced by the cost of the front ITO electrode in that particular study.

Table 3. Manufacturing cost estimates for a perovskite stack and module, sourced from the literature.

The perovskite cell stack structure reported in the most recent study, by Song et al. [30], is closest to the stack described earlier, in the perovskite/c-Si tandem cell results section; the stack has a manufacturing cost estimate, including the monolithic interconnected semi-transparent stack with busbars, of about $9±1/m². However, that study assumes a stack of unproven simplicity, without the use of organic charge transfer materials. The same study notes that the current cost of several often-used organic layers (e.g. PCBM) is excessive. Thus, in principle a perovskite stack cost consistent with a significant cost/Wp reduction (see Fig. 10) is feasible, although a challenge may still present itself in relation to other additional tandem costs, such as for barriers to ensure the stability of the perovskite cell stack, or an increase in cost/Wp associated with the junction box, system cabling or electronics.

Conclusions

The perovskite/c-Si tandem concept is considered to be very promising for significantly enhancing the mainstream module efficiency. The increased energy yield versus the nominal increase in manufacturing cost per m² is expected to result in a decrease in LCOE. Besides the high potential suggested by the calculations, a few research groups, including ECN/Solliance, have made significant progress in experimental demonstrations of high-efficiency tandem cells in recent years.

In terms of efficiency results, the perovskite/c-Si tandem has caught up with the world record of the SJ c-Si cells after just a few years of development. To further increase the tandem cell efficiency, to beyond 30%, special attention must be paid to the reduction of optical losses and to the optimization of the perovskite band gap.

In order to actually commercialize the perovskite/c-Si tandem technology, reliability and scalability of perovskite technologies are extremely important aspects. With optimized cell architecture and encapsulation, perovskite cells have demonstrated considerable progress in stability under continuous illumination and thermal stress. Furthermore, it was found that perovskite cells processed by scalable technologies, such as slot die coating, can perform just as well as those processed by lab-scale spin coating.

Acknowledgements

> **"Reliability and scalability of perovskite technologies are extremely important aspects."**

of Jinko Solar for the commercial PERC and Al-BSF cells for performance analysis in the tandem stack.

....

References

[1] ITRPV 2018, "International technology roadmap for photovoltaic (ITRPV): 2017 results", 9th edn (Mar.) [http://www.itrpv.net/Reports/Downloads/].

[2] Zhang, E.D. et al. 2016, "Combination of advanced optical modelling with electrical simulation for performance evaluation of practical 4-terminal perovskite/c-Si tandem modules", *Energy Procedia*, Vol. 92, pp. 669–677.

[3] Löper, P. et al. 2015, "Organic–inorganic halide perovskite/crystalline silicon four-terminal tandem solar cells", *Phys. Chem. Chem. Phys.*, Vol. 17, pp. 1619–1629.

[4] Yu, Z. (Jason), Leilaeioun, M. & Holman, Z. 2016, "Selecting tandem partners for silicon solar cells", *Nat. Energy*, Vol. 1, p. 16137.

[5] Eperon, G.E., Hörantner, M.T. & Snaith, H.J. 2017, "Metal halide perovskite tandem and multiple-junction photovoltaics", *Nat. Rev. Chem.*, Vol. 1, p. 95.

[6] Omar Ramirez Quiroz, C. et al. 2018, "Balancing electrical and optical losses for efficient 4-terminal Si-perovskite solar cells with solution processed percolation electrodes", *J. Mater. Chem. A*, Vol. 6, pp. 2583–3592.

[7] McGehee, M. & Holman, Z. 2018, Announcement at the MRS Spring Meeting.

[8] Green, M.A. et al. 2017, "Solar cell efficiency tables (version 50)", *Prog. Photovolt: Res. Appl.,* Vol. 25, pp. 668–676.

[9] Najafi, M. et al. 2018, "Highly efficient and stable flexible perovskite solar cells with metal oxides nanoparticle charge extraction layers", *Small*, Vol. 14, 1702775.

[10] Zhang, D. et al. 2018 [submitted], "High efficiency 4-terminal perovskite/c-Si tandem cells", *Sol. Energy Mater. Sol. Cells.*

[11] Najafi, M. et al. 2018 [forthcoming], "Stable and highly transparent perovskite cell and module for high efficiency perovskite/c-Si 4-terminal tandems", 35th EU PVSEC, Brussels, Belgium.

[12] Coletti, G. et al. 2016, "23% metal wrap through silicon heterojunction solar cells – A simple technology integrating high performance cell and module technologies", *Proc. 32nd EU PVSEC*, Munich, Germany, pp. 715–717.

[13] Werner, J. et al. 2016, "Efficient near-infrared-transparent perovskite solar cells enabling direct comparison of 4-terminal and monolithic perovskite/silicon tandem cells", *ACS Energy Lett.,* Vol. 1, pp. 474–480.

[14] Rakocevic, L. et al. 2017, "Interconnection optimization for highly efficient perovskite

modules", *IEEE J. Photovolt.*, Vol. 7, No. 1, pp. 404–408.

[15] Galagan, Y. et al. 2016, "Towards the scaling up of perovskite solar cells and modules", *J. Mater. Chem. A*, Vol. 4, No. 15, pp. 5700–5705.

[16] Jaysankar, M. et al. 2018, "Perovskite-silicon tandem solar modules with optimised light harvesting", *Energy Environ. Sci.*

[17] Di Giacomo, F. et al. 2018, "Up-scalable sheet-to-sheet production of high efficiency perovskite module and solar cells on 6-in. substrate using slot die coating", *Sol. Energy Mater. Sol. Cells*, Vol. 181, pp. 53–59.

[18] Wang, J. et al. 2017, "Highly efficient perovskite solar cells using non☐toxic industry compatible solvent system", *Sol. RRL,* Vol. 1, 1700091.

[19] Jeon, N.J. et al. 2014, "Solvent engineering for high-performance inorganic–organic hybrid perovskite solar cells", *Nat. Mater.*, Vol. 13, pp. 897–903.

[20] Yanget, M. et al. 2017, "Perovskite ink with wide processing window for scalable high-efficiency solar cells", *Nat. Energy,* Vol. 2, 17038.

[21] Conings, B. et al. 2016, "A universal deposition protocol for planar heterojunction solar cells with high efficiency based on hybrid lead halide perovskite families", *Adv. Mater.,* Vol. 28, No. 48, pp. 10701–10709.

[22] Solliance 2018, Press release (Apr.) [https://solliance.eu/nl/solliance-sets-14-5-cell-performance-record-on-large-perovskite-modules/].

[23] Bush, K.A. et al. 2017, "23.6%-efficient monolithic perovskite/silicon tandem solar cells with improved stability", *Nat. Energy,* Vol. 2, 17009.

[24] Richter, A. et al. 2017, "n-Type Si solar cells with passivating electron contact: Identifying sources for efficiency limitations by wafer thickness and resistivity variation", *Sol. Energy Mater. Sol. Cells,* Vol. 173, pp. 96–105.

[25] Haase, F. et al. 2017, "Interdigitated back contact solar cells with polycrystalline silicon on oxide passivating contacts for both polarities", *Jpn. J. Appl. Phys.,* Vol. 56 [https://isfh.de/en/26-1-record-efficiency-for-p-type-crystalline-si-solar-cells/]

[26] Luxembourg, S.L. et al. 2017, "Perovskite/crystalline silicon tandems: impact of perovskite band gap and crystalline silicon cell architecture", *Proc. 33rd EU PVSEC*, Amsterdam, The Netherlands, pp. 1176–1180.

[27] Geerligs, L.J. et al. 2018 [forthcoming], "PERC and nPERT industrial low-cost cells provided with front polysilicon passivated contact for tandem application", 35th EU PVSEC, Brussels, Belgium.

[28] Stodolny, M.K. et al. 2017, "Material properties of LPCVD processed n-type polysilicon passivating contacts and its application in PERPoly industrial bifacial solar cells", *Energy Procedia,* Vol. 124, pp. 635–642.

[29] Geerligs, L.J. 2017, "On cost-effectiveness of perovskite/c-Si tandem PV systems", *Proc. 33rd EU PVSEC*, Amsterdam, The Netherlands, pp. 1171–1175.

[30] Song, Z. et al. 2017, "A techno economic analysis of perovskite solar module manufacturing with low-cost materials and techniques", *Energy Env. Sci.,* Vol. 10, pp. 1297–1305.

[31] Cai, M. et al. 2017, "Cost-performance analysis of perovskite solar modules", *Adv. Sci.,* Vol. 4, 1600269.

[32] Tinker, L. 2015, "Challenges and opportunities for organic-inorganic halide perovskite solar cells", Presentation, USA DOE Sunshot Initiative.

....

About the authors

Dong Zhang received his Ph.D. from Delft University of Technology, studying silicon heterojunction solar cells. In 2013 he joined ECN and Solliance as a researcher, working on thin-film solar cells. Currently, his main research interest is the tandem PV concept, combining perovskite and silicon technologies.

Stefan L. Luxembourg received his Ph.D. from AMOLF in the field of biophysics. After a postdoctorate on thin-film silicon at the Delft University of Technology, he joined ECN in 2009, initially in the field of policy studies. In 2013 he joined the ECN solar department, where he has been working on topics related to light management, down-conversion, colour generation and perovskite/silicon tandems.

S.C. (Sjoerd) Veenstra received his Ph.D. from the University of Groningen, The Netherlands. In 2002 he joined ECN to work on organic photovoltaics; this work then became part of Solliance in 2011, when the thin-film PV activities of imec, ECN and TNO were amalgamated in a 'solar alliance'. Since 2018 he has been the manager of Solliance's perovskite solar cell programme.

L.J. (Bart) Geerligs has been with ECN (now 'ECN part of TNO') since 2000, where he has since set up several research programmes. From 2004 to 2011 he was in charge of n-type cell technology projects, including the transfer to industrial pilot production of nPERT and nMWT technologies. Beginning in 2014 and for several years after, he led research on polySi passivating contacts, and is currently the programme manager for hybrid tandem solar cells and modules.

....

Enquiries

Bart Geerligs
Tel: +31 650 009 558
Email: bart.geerligs@tno.nl